Meteorol. Z. (Contrib. Atm. Sci.), Vol. 34 (2025), 293–306
Published online January 7, 2026

Open Access
Environmental Meteorology

Earlier harvest but more hail – hail risk to winter wheat in Switzerland since 1972

Raphael Portmann[1,*], Lukas Valentin Graf[2,3], Lena Wilhelm[4], Dario Fossati[5], Timo Schmid[2,6], Leonie Villiger[2,6], Pierluigi Calanca[1]

[1] Agroscope, Climate and Agriculture, Zurich, Switzerland
[2] ETH Zurich, Crop Science, Institute of Agricultural Science, Zurich, Switzerland
[3] Agroscope, Earth Observation of Agroecosystems Team, Division Agroecology and Environment, Zurich, Switzerland
[4] University of Bern, Oeschger Centre for Climate Research, Bern, Switzerland
[5] Agroscope, Field-Crop Breeding and Genetic Resources, Nyon, Switzerland
[6] Federal Office of Meteorology and Climatology MeteoSwiss, Zurich, Switzerland
[*] Corresponding author: raphael.portmann@alumni.ethz.ch

With 10 figures

Abstract: Winter wheat, the primary grain grown in Switzerland plays a crucial role for domestic food security. It is typically harvested in July and early August, roughly coinciding with the peak of the hail season. Recent global warming has led to earlier harvest dates, thus shortening the time window during which wheat is potentially exposed to hail. At the same time, the frequency of hailstorms in Switzerland has increased. In view of these two opposing trends, the question arises as to whether the risk of hail damage to wheat has decreased or increased over the past few decades. To address this question and evaluate the relative importance of the two trends, we combined wheat phenology simulated with the World Food Studies (WOFOST) model with a reconstruction of the seasonal distribution of hail days over the periods 1972–1991 and 2002–2021. We find that across Switzerland, harvest dates advanced by an average of 13.4 days between 1972–1991 and 2002–2021, while the mean number of hail days during wheat's growing season increased from 0.79 to 1.12. Thus, while early harvests have potentially reduced hail risk by 13%, the significant 55% increase in hail frequency has offset this benefit, resulting in a net 42% increase in hail risk. It is beyond doubt that efforts are needed to enhance the agricultural sector's resilience against increasing hail damage risks. Our findings emphasize the importance of quantitative assessments that combine the development of hail scenarios, on the one hand, and crop growth modeling, on the other.

Keywords: hail damage; wheat; phenological modelling; radar data; climate change; risk modeling

1 Introduction

In Switzerland, as in other parts of Europe and the world, hail is a major threat to agricultural production (Schiesser 1990; Kopp et al. 2022; Portmann et al. 2024). The Swiss hail season starts in April, peaks in July, and ends in September (Nisi et al. 2016; Schroeer et al. 2022), aligning with the growing season of most major crops. Winter wheat grain setting, formation and ripening occur during June and July. Physiological maturity is reached around mid of July, while harvest typically takes place at the end of July, beginning of August. Important phenological stages are therefore critically exposed to the risk of damage through hail. Winter wheat constitutes Switzerland's main cereal crop, contributing approximately 50% of national cereal production (Swiss Granum 2023).

It is well established that the increase in temperature caused by climate change accelerates the phenological cycle of wheat and other annual crops (Menzel et al. 2006; Olesen et al. 2012; Mo et al. 2016). There is evidence that the anthesis (flowering) and maturity dates of winter wheat have advanced several days per decade in different regions of the world (Mo et al. 2016; Rezaei et al. 2018). This trend is projected to continue in the future (Olesen et al. 2012). This temperature-driven phenological advancement can, at least partially, reduce heat stress during anthesis (Rogger et al. 2021). It may also help wheat avoid periods of water shortage (Le Roux et al. 2024) or reduce the risk of pests and pathogens during flowering (Sheehan & Bentley 2021) and could also reduce the time window in which wheat can be damaged by hail.

The role of climate change on hail occurrence and associated crop damaging potential is complex as several factors

DOI: 10.1127metz/1263
Gebrüder Borntraeger Science Publishers, Stuttgart, www.borntraeger-cramer.com

play a key role (Raupach et al. 2021). Thermodynamically, large hailstones in individual storms are expected to become more frequent under climate change due to stronger updrafts and increased moisture availability. High-resolution model experiments of individual storms support this expectation (e.g. Mallinson et al. 2024). In addition, recent Europe-wide convection permitting simulations over a full decade show that hail frequencies are expected to decrease over Southwestern Europe and increase in Central and Northeast Europe, including Switzerland (Thurnherr et al. 2025). Detailed observational records of hailfall in time and space in Switzerland have been available only since 2002 (Schroeer et al. 2022) and past hail trends have often been assessed based on proxies, i.e. statistical relationships between atmospheric reanalysis or satellite imagery and hail occurrence (Punge et al. 2017; Raupach et al. 2023; Wilhelm et al. 2024). Using such an approach, Wilhelm et al. (2024) found a significant positive trend in the number of annual hail days in Switzerland, amounting to roughly 3–4 additional days per decade from 1959 to 2022. This suggests that the risk of hail damages to wheat could have increased in spite of earlier harvest dates.

Here, we address this hypothesis in quantitative terms. We evaluate changes in wheat phenology and hail occurrence since 1972 and examine their implications for the risk of hail damages to wheat in Switzerland. We employ a crop growth model to simulate winter wheat harvest dates over the past 50 years at 1 × 1 km spatial resolution. The modeled harvest dates are then combined with a radar-based climatology of crop-damaging hail for 2002–2021 (Schroeer et al. 2022; Portmann et al. 2024) and a recent multi-year reconstruction of hail events in Switzerland by Wilhelm et al. (2024). This allows us to balance the risk reduction due to earlier harvest dates on the one hand, and the increased risk caused by more frequent hail events over the last 50 years on the other.

The remainder of this article is structured as follows. First, the phenological data and modeling approach as well as the hail data and risk quantification are introduced (Section 2). In Section 3.1, the results of the model calibration and validation are presented followed by a discussion of the modeled spatio-temporal characteristics of harvest dates in Section 3.2. Then, changes in hail risk for winter wheat in Switzerland since 1972 are presented, including the separate contributions of earlier harvests and increasing hail

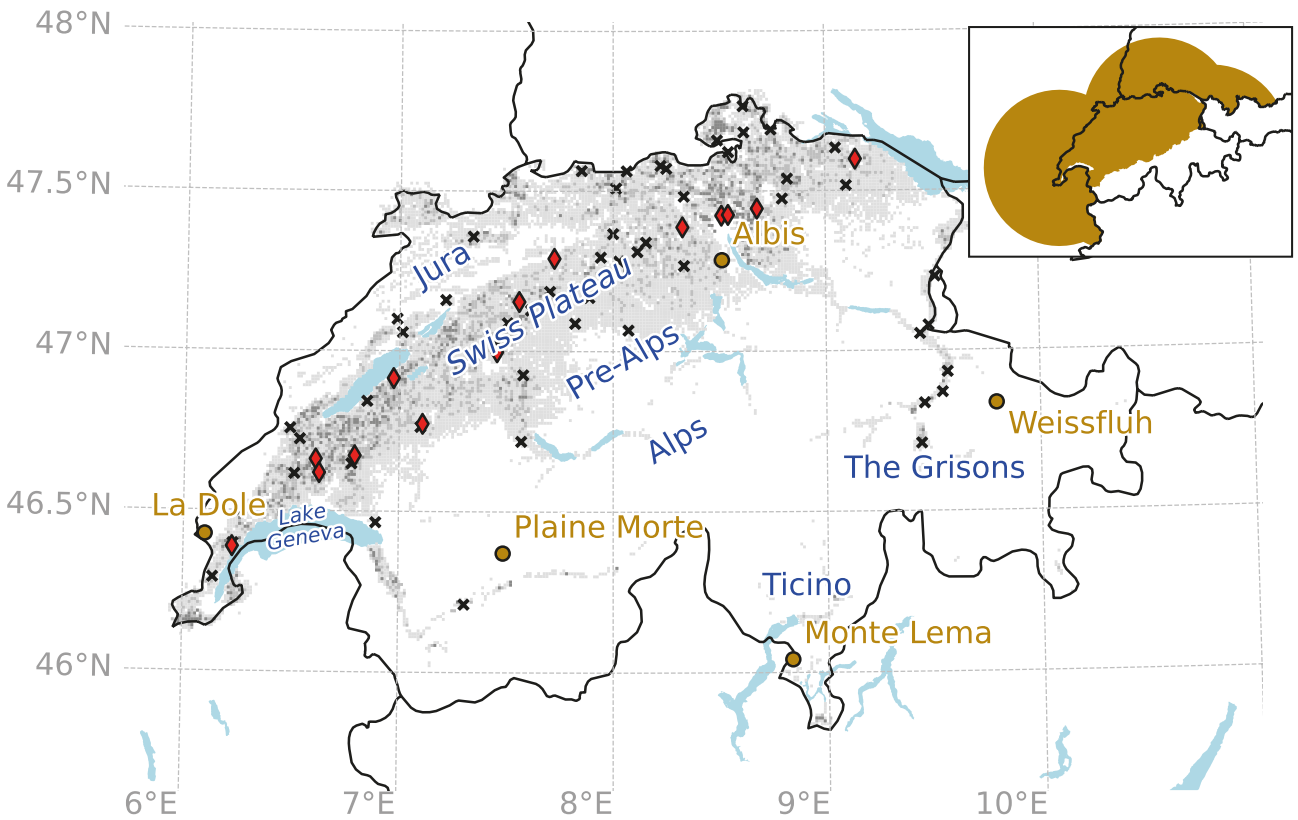

Fig. 1. Geographical map of the study region showing wheat field density (grey shading), sites of wheat field trials to calibrate the phenological model (red diamonds), locations of historical harvest observations (black crosses), and radar locations (brown circles). The inset at the top right shows the region for which Wilhelm et al. (2024) reconstructed historical hail days.

frequency in Section 3.3. This is followed by a discussion (Section 4) and conclusions (Section 5).

2 Material and methods

2.1 Wheat cultivation areas

To outline wheat production areas (Fig. 1) we used a gridded dataset at 1 × 1 km spatial resolution assembled by Portmann et al. (2024). The data contain the total number of fields and the total acreage of the four field crops wheat, barley, maize, and rapeseed and are valid for the year 2021. We assumed that the total acreage of the four crops is a good approximation of the wheat acreage, since wheat is the most important crop in Switzerland. We further assumed that the spatial distribution of the wheat cultivated area remained unchanged during the last decades. This assumption is questionable, but the lack of detailed spatial data extending back to the early 1970s precluded a more detailed reconstruction of the temporal evolution of the wheat cultivation area.

2.2 Phenological data

Data on wheat heading and harvest dates for the calibration of the phenological model were obtained from the records of the preliminary field trials of the Swiss federal agricultural research institute Agroscope/DSP breeding program and the official variety testing trials carried out across the Swiss Plateau (Fig. 1). These data were previously used by Rogger et al. (2021) in a study investigating the implications of climate change for heat stress in wheat. As our goal was not to precisely calibrate the phenological model for different varieties but rather to obtain a representative phenology, for the present analysis we considered only the wheat variety Arina. This variety was introduced in the early 1980s and has been cultivated ever since, reaching a share of the wheat cropping area of approximately 70% in the late 1980s and 1990s (Fossati & Brabant 2003). Phenological data for this variety were available for 14 locations and 19 years (2000–2018) (Fig. 1). The data were geocoded as day-of-year (DOY) at postcode level, as the exact location of the test sites was not disclosed.

Completely independent phenological data for model verification were extracted from the database of the Swiss Federal Office of Meteorology and Climatology (MeteoSwiss). The data originate from a network established by MeteoSwiss in the 1950s to monitor plant phenology in both wild plants and crops. However, phenological observations on crops were discontinued in 1996 (Defila et al. 2016). Data collected for our work contain harvest dates from 74 locations (Fig. 1) covering the period between 1972 and 1995, with time records spanning between 1 and 24 years, depending on location.

2.3 Modeling wheat phenology

To simulate the development of winter wheat, we opted for the WOrld FOod STudies (WOFOST) model. In WOFOST, the developmental rate of wheat is modeled as a crop- and cultivar specific function of ambient temperature, modified by a factor that depends on length of day, which is relevant for crops characterized by photosensitive developmental stages, such as wheat (Wit et al. 2019). The model tracks the phenological evolution using a dimensionless state variable DVS (development stage) which, for annual crops, takes a value of 0 at seedling emergence, a value of 1 at flowering and a value of 2 at maturity (Ceglar et al. 2019). We assumed harvest to occur at maturity, although it is important to note that in practice these two events do not necessarily match, especially when unfavorable weather prompt farmers to anticipate or delay the harvest.

Following Graf (2024), we calibrated WOFOST's phenology by optimizing the effective temperature sum needed to reach the heading stage ($T_{sum}1$) and the effective temperature sum needed to reach physiological maturity ($T_{sum}2$). All other model parameters were extracted from the Python Crop Simulation Environment (PCSE) database specifying the "Winter_Wheat_105" parameter set as target. We first calibrated $T_{sum}1$ within a parameter interval of 700 °C to 900 °C by minimizing the root-mean square error (RMSE) between modeled and observed heading dates. Next, we calibrated $T_{sum}2$ within a parameter interval of 950 °C to 1050 °C, choosing the optimal value $T_{sum}1$ from the first calibration step to initialize the temperature accumulation between heading and maturity. Both calibration steps were implemented using the Powell bound-constrained optimizer from "scipy.optimize.minimize" in Python 3.10.

After calibration, we ran WOFOST on all 1 × 1 km grid cells assigned to wheat cropping as described in Section 2.1 (n = 12717). The simulations spanned 50 consecutive growing seasons from 1972 to 2021. The same sowing date (October 15) was prescribed in all years. This choice is based on Graf (2024), who demonstrated that, owing to the effects of vernalization, spring and summer phenology are unaffected (≤ 1 day) by moderate shifts in sowing date. If maturity was not reached after 330 days, the simulation was stopped and the harvest date set to a missing value.

Daily data of the minimum ($T_{min}d$) and maximum ($T_{max}d$) temperature at 1 × 1 km spatial resolution required as input to WOFOST were extracted from the spatial climate analyses obtained from MeteoSwiss. The latter were developed by statistical interpolation of weather station measurements, taking into account topographic effects (Frei 2014).

2.4 Hail occurrence

We derived a daily climatology of crop-damaging hail days for 2002–2021, following the approach of Portmann et al. (2024). This method is based on the operational C-band radar data from MeteoSwiss's five operational radar stations (Fig. 1) and uses the Maximum Expected Severe Hail Size (MESHS) as a proxy for hail occurrence (Witt et al. 1998). Following the recommendation in Portmann et al. (2024), we adopted a MESHS threshold of 34 mm to identify crop-

damaging hail situations. The threshold of 34 mm minimizes the frequency bias (i.e., the over- or underprediction of damages), which is particularly relevant for climatological analyses as performed here. Further, we reduced the spatial resolution from 1 × 1 km to 8 × 8 km to increase the robustness of our estimates (Fig. 2a) and applied a 61-day running filter to smooth the resulting climatology at each grid point (Fig. 2b). According to Portmann et al. (2024), coarsening the spatial resolution of MESHS to 8 km yields better skill in modeling the occurrence of hail damage compared to 1 km mainly because uncertainties in the radar data, e.g., due to horizontal hail drift are better accounted for.

Since spatially explicit information on hail was not available for the years before 2002, we inferred a climatology of crop-damaging hail days for 1972–1991 by multiplying the radar based climatology for 2002–2021 with a constant conversion factor to account for the increase in hail days over the last decades. We determined the latter based on the statistical reconstruction of hail days for Switzerland by Wilhelm et al. (2024), which covers the period 1959–2022. This dataset contains a daily time series of hail occurrence valid for whole Northern Switzerland. To compute the conversion factor, we first evaluated the mean seasonal distribution of hail days for each of the two periods in question (1972–1991 and 2002–2021), smoothed the resulting curves with a 61-day running filter, integrated over time to derive the cumulative numbers of hail days, and computed daily ratios of the cumulative hail days (1972–1991 against 2002–2021). The procedure is illustrated in Fig. 3. As seen in this figure, for DOY > 120, the daily ratios do not vary significantly, allowing us to adopt an average conversion factor of 0.62 (DOY 120 to 274).

2.5 Assessing hail risk

To assess hail risk (d), we used the total number of crop-damaging hail days from the start of the hail season (April 1) to the modeled harvest date. We evaluated this measure at each grid-point by integrating the corresponding smoothed seasonal distribution of hail probabilities. We first calculated the total change in risk, Δd_{tot}, as the difference between total number of hail days during the growing-season of the years 2002–2021 and total growing-season hail days of the years 1972–1991, and then partitioned this total risk change into a contribution from the change in harvest date, Δd_{hvst}, and a contribution associated with increasing probability of hail, Δd_{hail}. As illustrated in the schematic representation in Fig. 4, the total risk during the first period (1972–1991) is given by:

$$d_{\mathrm{past}} = d^{*} + \Delta d_{\mathrm{hvst}} \tag{2.1}$$

(the sum of the grey and blue areas in the first panel of this figure) whereas the total risk during the second period (2002–2021) is given by:

$$d_{\mathrm{pres}} = d^{*} + \Delta d_{\mathrm{hail}} \tag{2.2}$$

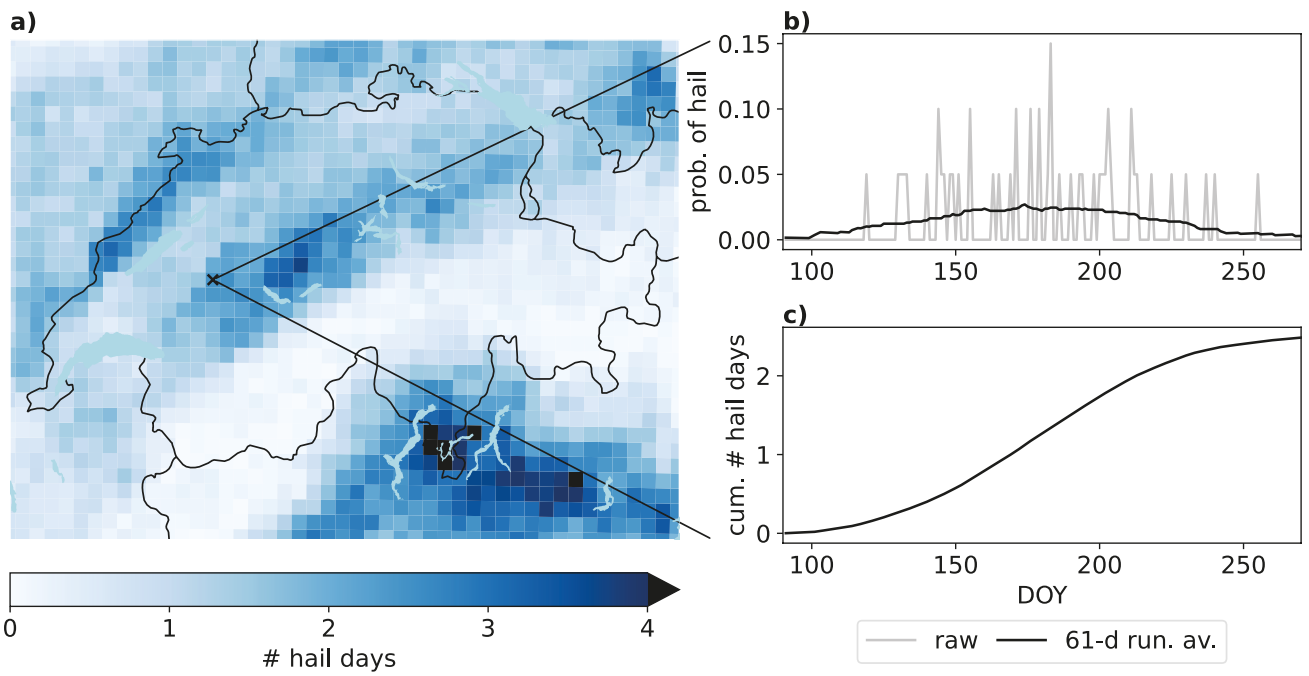

Fig. 2. (a) Annual number of crop-damaging hail days at 8 km averaged over the period 2002–2021, (b) raw (grey) and the smoothed climatology using a 61-day running average (black) of the daily probability of hail at the grid point marked with a black cross in panel (a), and (c) cumulative number of hail days at that grid point.

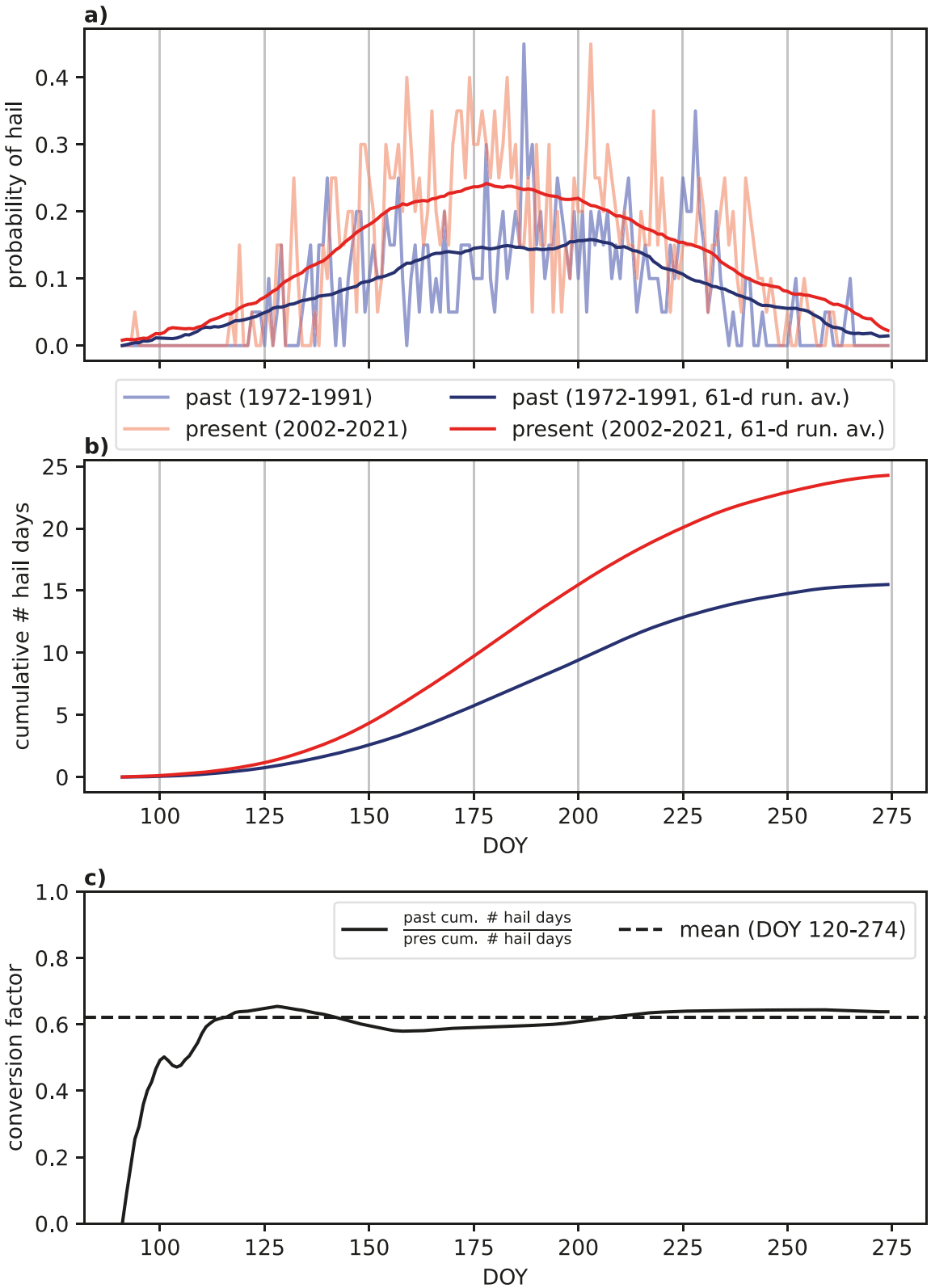

Fig. 3. (a) Annual average number of hail days (light colors) and a 61-day running average (dark colors) North of the Alps for the past period 1972–1991 (blue) and the present period 2002–2021 (red). (b) The same as (a) but cumulative number of hail days. (c) Cumulative number of hail days for 1972–1991 divided by cumulative hail days 2002–2021 (conversion factor) derived from unsmoothed annual averages (grey) and 61-day running average (black).

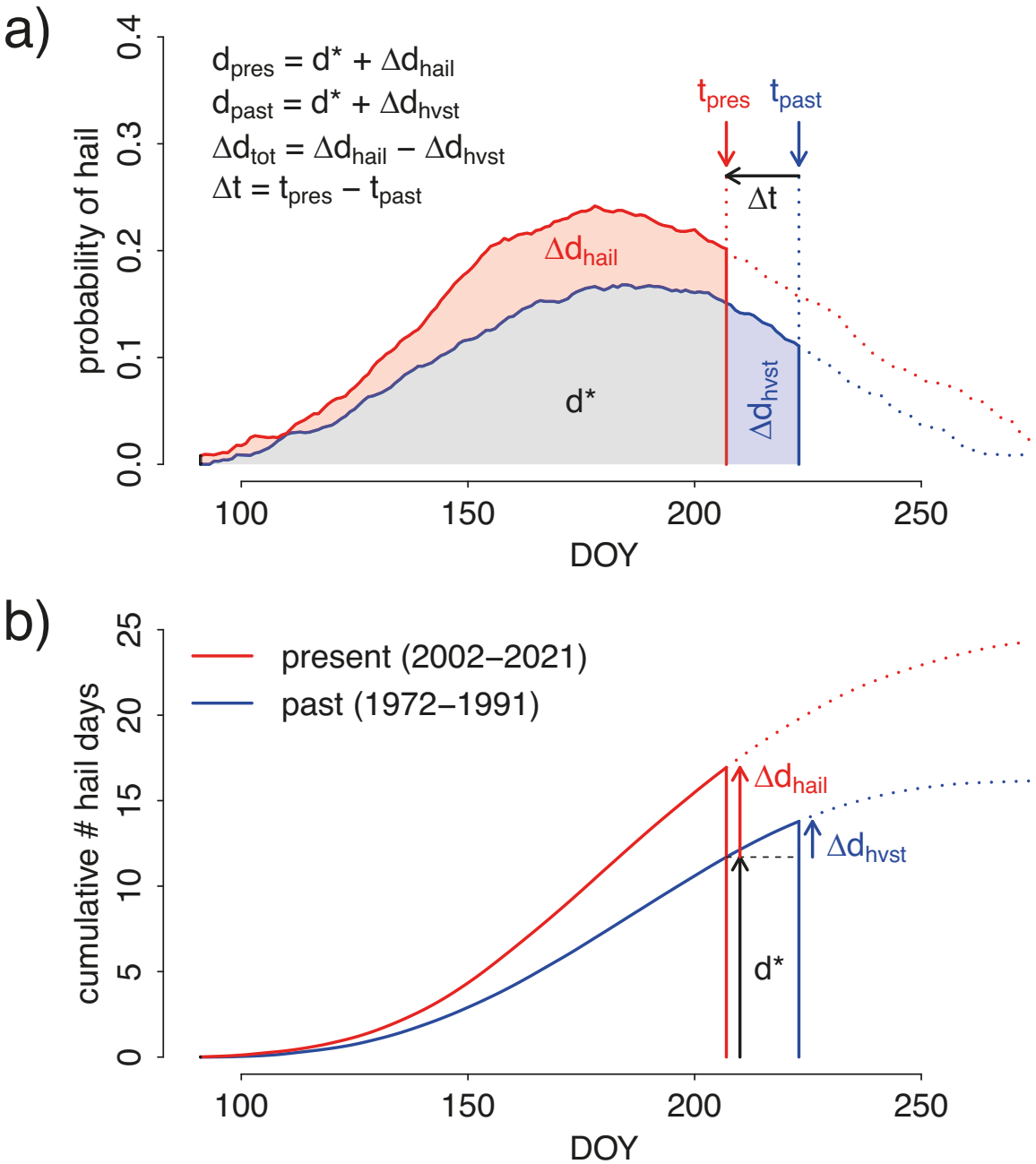

Fig. 4. Schematic depiction of the quantification of risk in this study showing (a) daily probabilities of hail and (b) cumulative number of hail days at a grid point for the present (red) and the past (blue) periods. Risk is quantified as the time integral over the daily probabilities, i.e., the cumulative number of hail days until the harvest date and can be expressed as sum of the labeled areas in panel (a), see text for details.

(the sum of the grey and red areas). In these two equations, the grey area d^* represents the integral of the past (1972–1991) hail days up to the current (i.e., 2002–2021) harvest date. Hence, the change in risk between past (1972–1991) and present (2002–2021) is given by:

$$\Delta d_{tot} = d_{pres} - d_{past} = \Delta d_{hail} - \Delta d_{hvst} \quad (2.3)$$

which is what we intended to show. Eventually, all involved terms can be computed directly from the cumulative hail days at each grid point (Fig. 2c), as illustrated in Fig. 4b.

3 Results

3.1 WOFOST calibration and validation

The calibration of the phenology module in WOFOST with data from field trials gave values of 832 °C for $T_{sum}1$ and 973 °C for $T_{sum}2$. Calibration results showed a coefficient of determination (R^2) of 0.59, a bias (*BIAS*) of 0.5 days and root-mean square error (*RMSE*) of 5.4 days (Fig. 5a). Corresponding statistics obtained during model validation on the 1972–1995 data set from MeteoSwiss were of $R^2 = 0.57$, $BIAS = -2.7$ days and $RMSE = 9.0$ days, respectively (Fig. 5b). Factors that could explain the lower overall performance during validation are in particular the lack of information concerning varietal choices and other management decisions as well as lack of information concerning data collection protocols and data quality control during the earlier collection phase of these verification data. Furthermore, validation results showed considerable variation across sites: locations in Western Switzerland are mostly characterized by a good model performance (R^2 0.7, *RMSE* 5 days), while sites in Central and Eastern Switzerland showed less satisfactory model performance ($R^2 < 0.4$, $RMSE > 5$ days) (not shown). Again, this could be due to diverging varietal choices and management practices in different regions.

3.2 Temporal evolution of wheat harvest

Averaged across all grid cells, there was a clear shift to earlier harvests over the past 50 years (Fig. 6), with harvest occurring 13.4 days earlier in 2002–2021 than in 1972–1991. In addition to the trend, Fig. 6 suggests that there were substantial geographical variations in harvest dates (variability range in grey in this figure), amounting to a time-averaged (1972–2001) spatial standard deviation of 7.6 days.

Next, consideration is given to the geographical patterns of harvest dates as well as their long-term shifts (Fig. 7). Focusing on the past period (Fig. 7a), regions with earlier and regions with later harvest dates can be identified. As discussed in Graf (2024) in relation to wheat heading dates, these spatial patterns mainly emerge as a result of topography: Earlier harvest dates are found in warmer regions at lower elevations, and later harvest dates in colder regions at higher elevations.

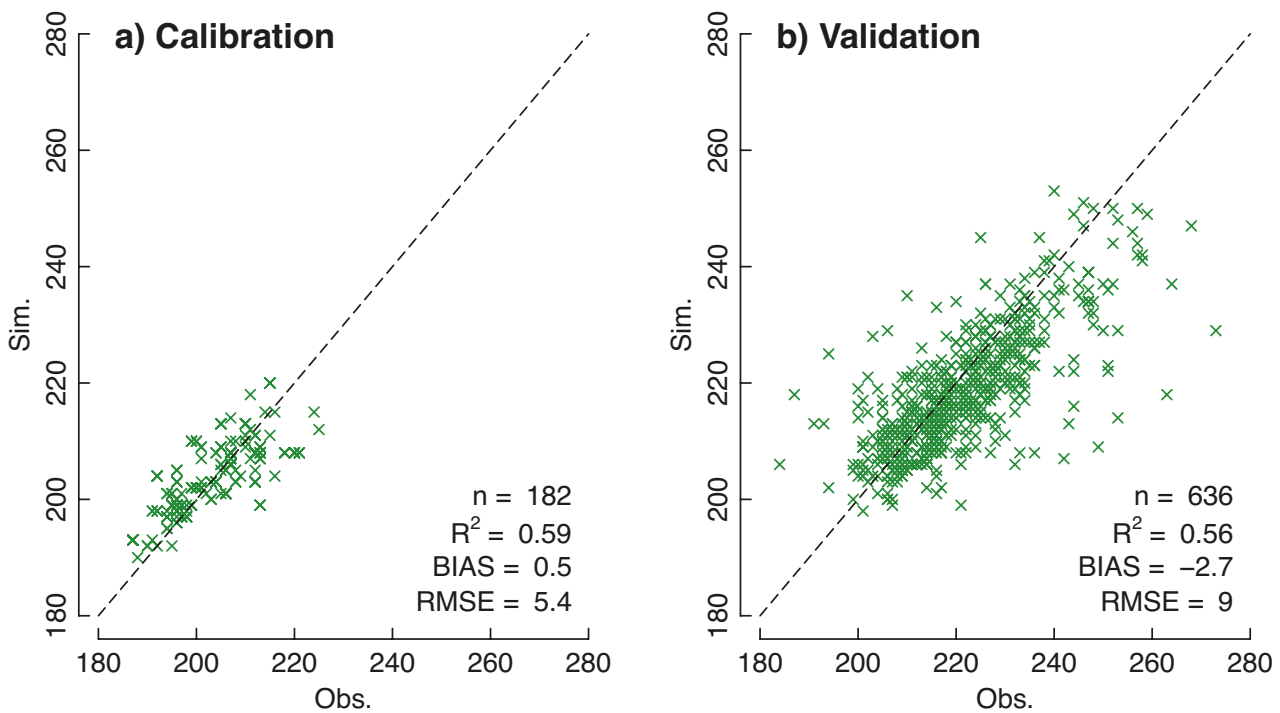

Fig. 5. Simulated vs. observed wheat harvest dates for (a) model calibration with data from field trials and (b) model validation with MeteoSwiss phenological observations.

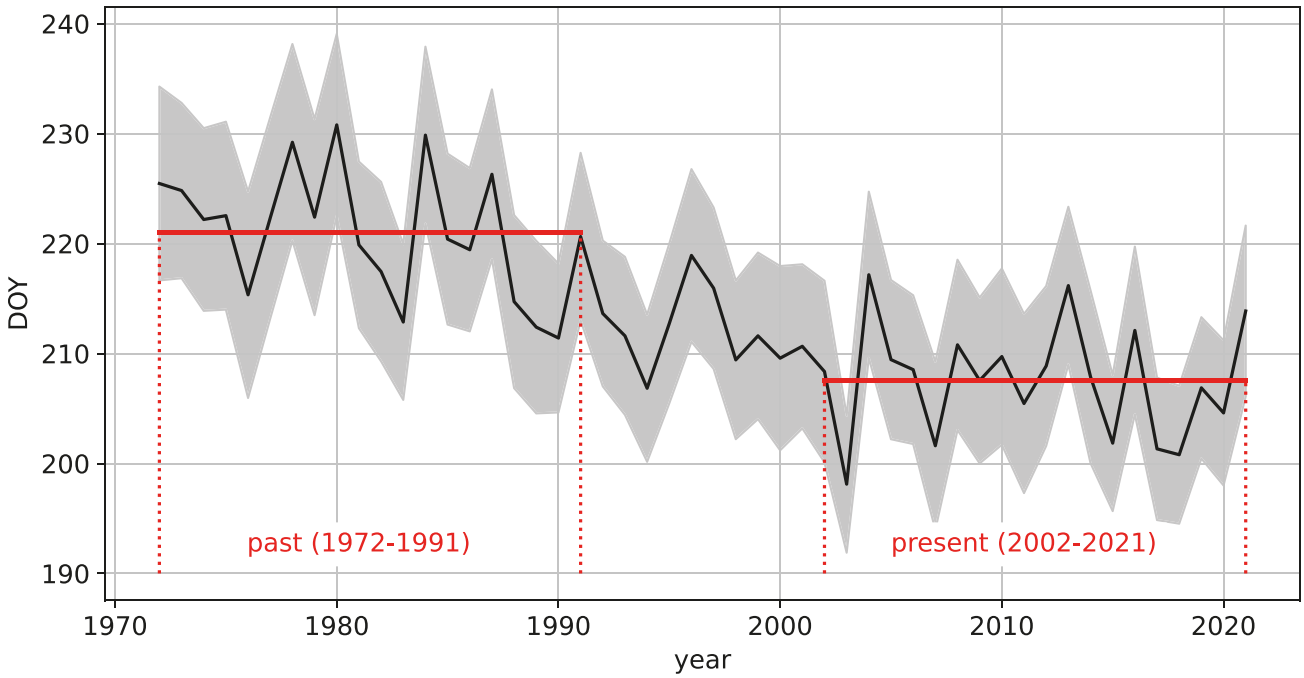

Fig. 6. Mean (black line) and standard deviation (gray shading) of modeled harvest dates considering all grid points for the period 1972–2021. Red horizontal lines indicate the average harvest date for the past (1972–1991) and the present (2002–2021) reference periods used in this study.

Similar patterns appear also in the spatial distribution of harvest dates for the more recent time window (Fig. 7b).

Focusing on the change in harvest dates between the two periods (Fig. 7c), we find distinct spatial patterns in the overall advancement in relation to heading dates. Graf (2024) pointed out that the trend is a function of elevation, because in colder regions at higher elevations the warming that occurred since the early 1970s was stronger than in warmer regions at lower elevations, resulting in a stronger advancement in harvest dates at higher locations. Accordingly, the advancement varied from 4–6 days over the main central Plateau to more than 20 days in the hill zone of the Pre-Alpes. These results emphasize the importance of accounting for the spatial variation of harvest dates in assessing hail risk.

3.3 Hail risk

Combining modeled harvest dates with the climatological hail frequencies (Section 2.4) as outlined in Section 2.5 yields geographical distributions of past (1972–1991) and present (2002–2021) hail risk, d_{past} and d_{pres}, respectively, as presented in Fig. 8. Both maps indicate large hail risk along the Pre-Alps and in the Jura mountains, with values of around 1.5–2.0 hail days during 1972–1991, and 2–2.5 hail days during 2002–2021. These regions are characterized by a combination of late harvest dates due to colder temperatures at higher elevations and frequent hail occurrence. High values of hail risk are also found in Southern Switzerland (Ticino, 1–2.5 hail days during 2002–2021), a climatically mild region characterized by early harvest dates but high frequency of hail occurrence. In the belt extending from Lake Geneva to Northeastern Switzerland, low annual hail frequencies are combined with comparatively early harvests, resulting in low hail risk (< 1 hail days during 2002–2021). Hail risk is particularly low in the inner alpine valleys (Valais and the Grisons), mainly as a result of rare hail occurrence.

Visual comparison of the two maps in Fig. 8 suggests an increase in the number of hail days by about 0.5. A more detailed analysis of the change in hail risk and its causes is presented in Fig. 9. The total change in hail risk, Δd_{tot} (Fig. 9a), shows distinct geographical patterns with the largest changes in regions characterized by high hail risk. Note that this is an immediate result of estimating past hail frequencies with a spatially constant conversion factor (Section 2.4), which evidently produces large changes at locations with high hail frequencies. The risk reduction due to earlier harvests, Δd_{hvst} (Fig. 9b), also tends to be high in magnitude where hail frequencies are high (Pre-Alps, Jura, and Ticino). This matches the expectation from the definition of Δd_{hvst} as shown in Fig. 4. Overall, however, the total signal, Δd_{tot}, reflects the change in hail frequency, Δd_{hail}, with Δd_{hvst} only acting to slightly dampen the spatial structure imposed by Δd_{hail} (Fig. 9c). On average, hail risk has increased from 0.79 days during 1972–1991 to 1.12 days during 2002–2021. Increasing hail frequencies have added 0.43 days to hail risk, while earlier harvests have decreased it by 0.1 days over the same period.

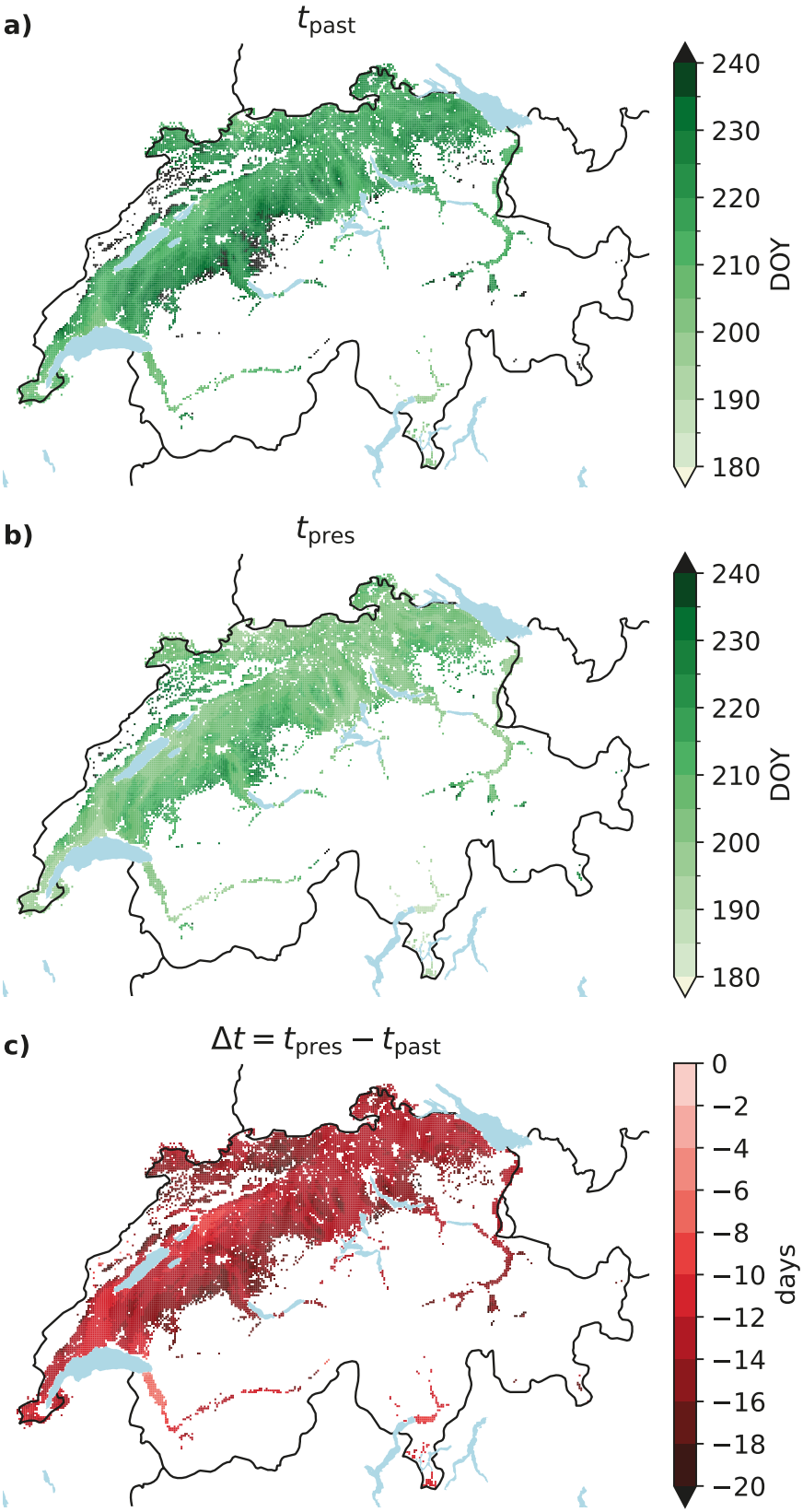

Fig. 7. Maps of the mean harvest dates for a) the past (1972–1991) and b) the present (2002–2021) period as well as c) the change between the two periods.

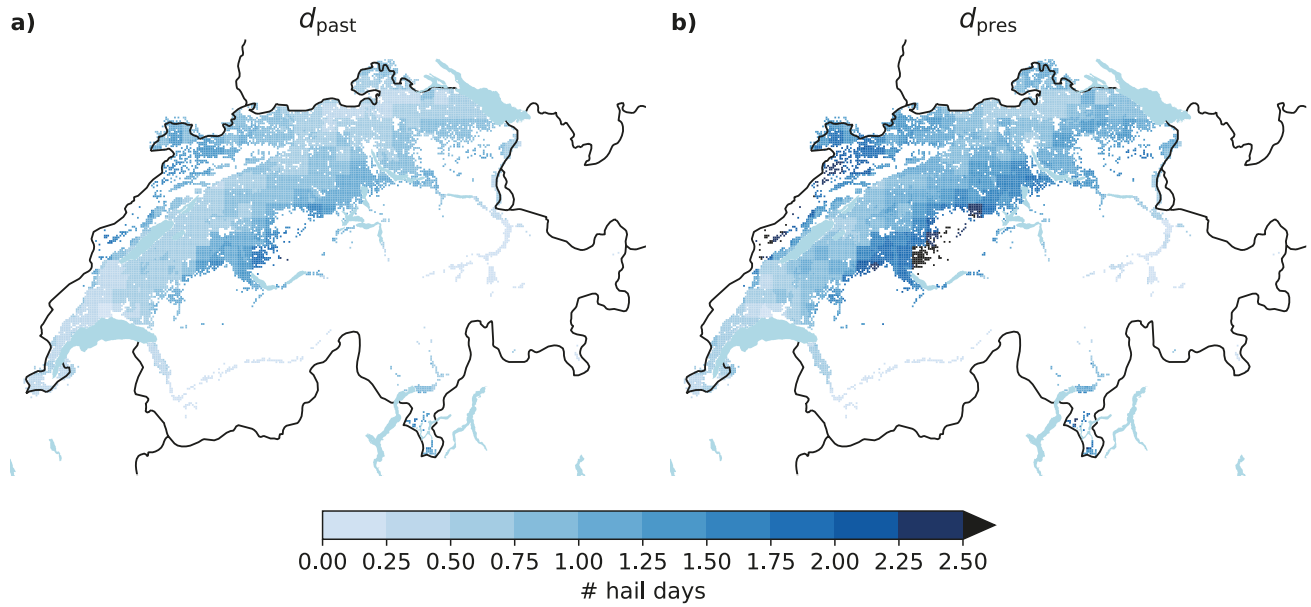

Fig. 8. Hail risk quantified as the mean number of crop-damaging hail days from the beginning of the hail season to harvest (d) for a) the past (1972–1991) and b) the present (2001–2021) period.

To better understand these latter results, in Fig. 10, we plot Δd_{hail}, Δd_{hvst} and Δd_{tot} as a function of both harvest date as well as hail risk. In this figure, isolines were added to the scatterplots using the same color scheme to aid interpretation. The isolines were obtained by running a simplified model, in which the seasonal distribution of hail days in Fig. 3 was approximated with a bell-shaped function (location parameter = 185, scale parameter = 37.5 days) and the shift in harvest date was modelled as a linear function of the harvest date (intercept = 22, slope = −0.17) based on a regression of the WOFOST output. In these plots, the distribution of points across the quadrant spanned by the x- and y-axes suggests a positive relationship between annual number of hail days and harvest date. This is because regions at higher elevations with later harvests (i.e., Pre-Alps, Jura) are also hail hotspots, while warmer, lower-lying regions with earlier harvests (Swiss Plateau, region around Lake Geneva) tend to be less hail-prone. A notable exception is the Ticino south of the Alps with high hail frequencies but early harvest dates, represented by the dots in the top left of the diagrams. Contrasting the points and isolines with respect to the colors indicates that the simiplified model captures the basic behaviour of Δd_{hail}, Δd_{hvst} and Δd_{tot} as a function of the harvest date and the number of hail days.

As seen in Fig. 10a, the increase in hail risk caused by the increase in hail frequency is larger for later harvest dates (longer growing season). The reduction in risk associated with the advancement of the harvest date (Δd_{hvst}, Fig. 10b) is larger for higher hail frequencies (given the same shift in harvest date, the blue area in Fig. 4a is larger the higher the overall probability of hail). For a given (annual) hail frequency Δd_{hvst} is shaped by two aspects (cf. the blue area in Fig. 4a): First, the shift in harvest date Δt is larger at sites with later harvests, contributing to an increase in Δd_{hvst}. Second and more important, Δd_{hvst} is larger the closer the harvest date is to the peak of the hail season. Hence, Δd_{hvst} peaks for harvest dates around DOY 200. Finally, as the total change in risk, $\Delta d_{tot} = \Delta d_{hail} - \Delta d_{hvst}$, is dominated by Δd_{hail}, the general trend observed in Fig. 10c for Δd_{tot} is similar, though slightly more pronounced, than the general trend observed in Fig. 10a for Δd_{hail}. For late harvest dates and high hail frequencies (top right of the diagram) the total change in risk depends roughly equally on both variables. For early harvest dates and high frequencies (top left), dependence on harvest date is larger than dependence on hail frequency. Finally, for low hail frequencies (bottom part) dependence on harvest date is very small.

4 Discussion

In this study, we examined the implications of the changes in wheat phenology and hail frequency over the past 50 years in Switzerland for the risk of hail damage to wheat, addressing in particular the question of whether shorter growing seasons associated with positive temperature trends may have contributed to reducing the hail risk of winter wheat. We found that despite the strong advancement of the harvest dates by about 2 weeks on average between 1972–1991 and 2002–2021, for a large fraction of the wheat cultivation area the accompanying reduction in hail risk was not enough to compensate for the increased risk due to more frequent hail occurrence over

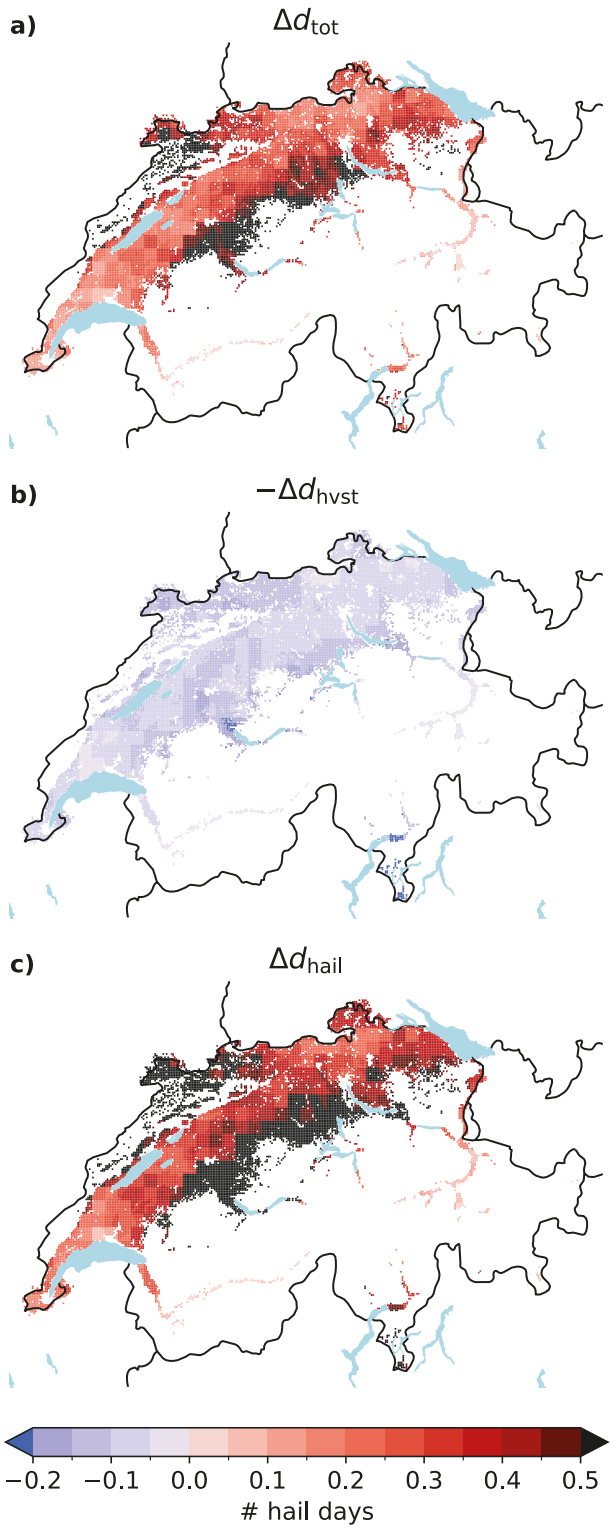

Fig. 9. Total change in hail risk from past to present (Δd_{tot}), the reduction due to earlier harvests ($-\Delta d_{hvst}$), and the increase due to more frequent hail occurrence (Δd_{hail}).

the same time period (roughly + 50%). We are not aware of any other study investigating the interplay between shifts in crop phenology and changes in climatic threats with respect to hail. Nonetheless, we note that earlier studies focusing on heat stress or water deficit also indicated that risk reduction induced by earlier harvests tends to be outweighed by increased frequencies of these hazards under climate change (e.g., Rogger et al. 2021; Le Roux et al. 2024).

Our findings are based on radar-derived hail frequencies, along with modeled harvest dates. Both, hail frequency estimates and simulated harvest dates are subject to uncertainties and assumptions, which are discussed in the following. First, the MESHS hail detection algorithm suffers from a large number of false alarms (e.g., Nisi et al. 2016; Schmid et al. 2024). We partly addressed this problem by aggregating the original signal to a coarser spatial resolution (decreasing it from 1 to 8 km) and by employing a MESHS detection threshold that yields a frequency bias of around one (Portmann et al. 2024). In this way, we were able to correct false alarms, at least on average. A similar approach was used by Warren et al. (2020).

Another important limitation of our study was the reconstruction of a hail climatology for the earlier period (1972–1991) by multiplying present hail frequencies (2002–2021) with a spatially constant conversion factor. This automatically generates large changes in hail frequencies in regions with frequent hail occurrence, which may not accurately reflect historical trends. Again, we can only stress the fact that the approach was dictated by the limited amount of historical data.

The conversion factor used to map the present spatial distribution of hail days into a past distribution of hail days was derived from the results of Wilhelm et al. (2024). Although these authors considered a slightly different hail detection algorithm (Probability Of Hail, POH) rather than MESHS in their analysis, we assumed that average changes in POH and MESHS frequencies are comparable. Our justification for this choice is that both radar products are derived from the radar signal in a similar way, i.e., by considering the difference between the height of melting level and the height a of a specified reflectivity level (Waldvogel et al. 1979). Although the details of the derivations are different, we expect that the conversion factor would not have differed substantially if the time series presented by Wilhelm et al. (2024) had instead been recalibrated using MESHS. Eventually, both radar algorithms capture severe hail days.

Turning to the modelling of harvest dates, a key limitation of our study is that only one wheat variety (Arina) was considered, while in practice cultivated wheat varieties have varied over time, with a tendency to favor early maturity varieties in recent years (Rezaei et al. 2018). Hence, it is possible that trends in harvest dates estimated in the present analysis are not fully representative of the actual trends in harvest dates that occurred in the recent past across the Swiss

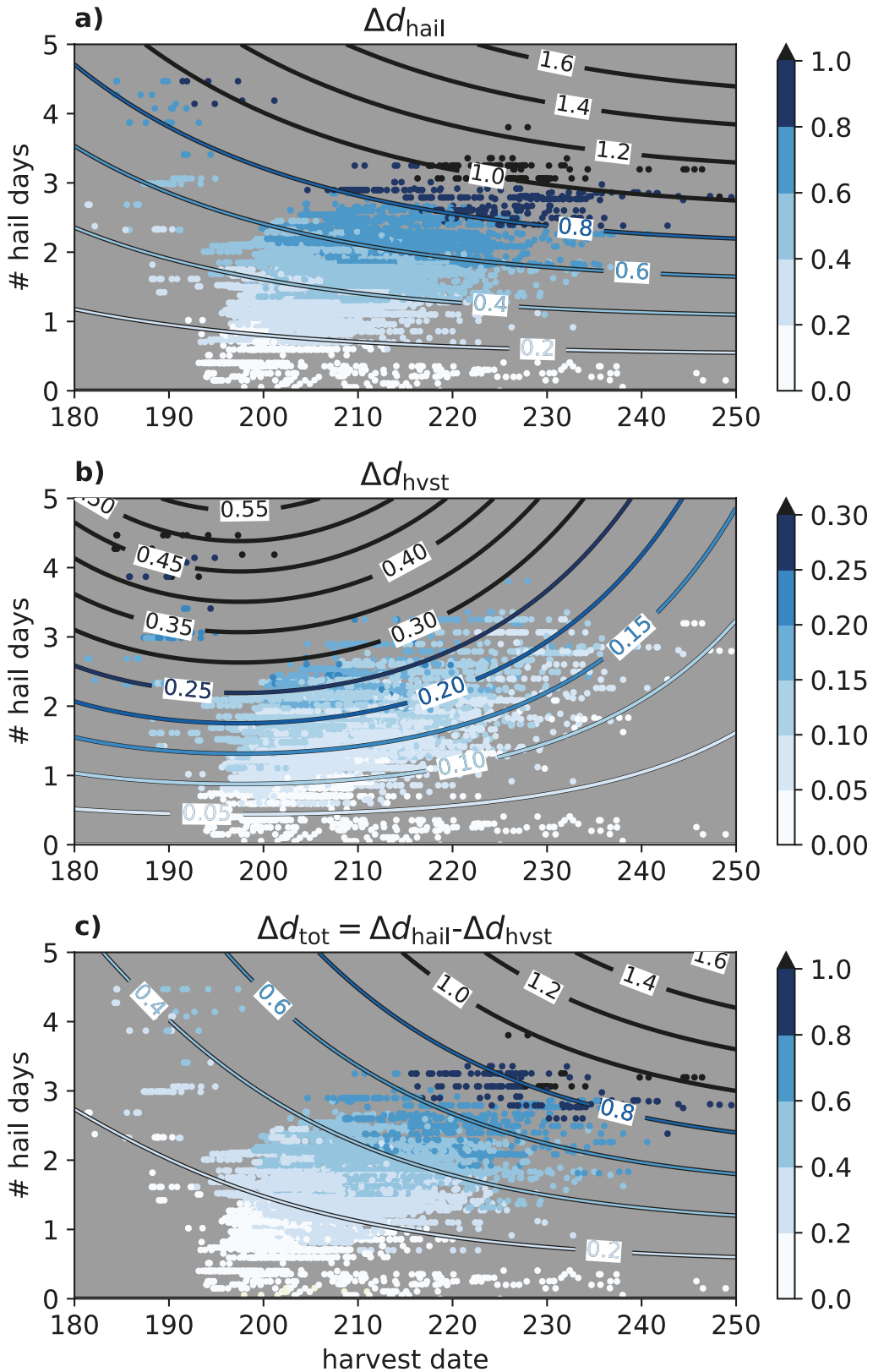

Fig. 10. Scatter plots showing total annual number of hail days as a function of present day wheat harvest dates (t_{pres} with dots coloured by (a) Δd_{hail} (b) Δd_{hvst}, and (c) $\Delta d_{tot} = \Delta d_{hail} - \Delta d_{hvst}$. The lines show the theoretical behaviour expected when the daily probability of hail is approximated with a Gaussian normal distribution and the change in harvest dates as a linear function of present day harvest dates.

territory. Further uncertainties concerning wheat phenology stem from the choice of running WOFOST with constant sowing date and standard values of the parameters controlling vernalization (i.e., exposure to cold temperatures providing the requirements for regrowth in spring). In reality, the latter also depend on wheat variety (Ceglar et al. 2019) and clearly further work is necessary to shed light on the impact of these approximations for the assessment of changing hail risk for wheat cultivation in Switzerland.

5 Conclusions

In Switzerland, advancement of wheat harvest dates observed during the past 50 years has reduced hail risk by 13% via a shortening of the time period during which wheat is exposed to hail. However, this was not sufficient to compensate for the concurrent 55% increase in hail frequency. Although we considered only one wheat variety (Arina) representing, at the time of writing, a small fraction of cultivated wheat varieties (less than 1.5% of sold seeds), we expect that the outcomes of our analysis are of general validity. Arina has been the main cultivar for at least two decades (see Section 2.2) and the heading date of current cultivars is on average only about 1.5 to 2 days earlier than Arina.

Because earlier harvest dates imply reduced exposure to hail, the introduction of early maturity wheat varieties that can be harvested earlier in the hail season could help partially prevent the risk of hail damage in wheat. A preliminary assessment of the potential benefits of early maturity varieties could be carried out with the help of the diagrams presented in Fig. 10. Our findings indicate that aiming for earlier harvests could be particularly interesting in regions where harvests occur during the peak of the hail season and where hail frequencies are high. In Switzerland this is the case in warmer regions at lower elevations, notably in Ticino.

To conclude, we provide a methodological framework to quantify hail risk on the background of climate-induced changes in cropping season duration. The approach can in principle be applied to other regions, crops, and meteorological hazards. Moving forward, we plan to extend the present analysis to integrate a novel set of highly resolved climate change simulations that should provide an improved representation of hail occurrence under global warming. We expect such assessments to be crucial to inform adaptation efforts in crop production and the insurance sector.

Data and code availability: Modeled harvest dates and code to analyze the data and produce the figures are available upon request from Raphael Portmann raphael.portmann@alumni.ethz.ch. The code to model harvest dates can be found on Zenodo (https://doi.org/10.5281/zenodo.17162414. We used PCSE Version 5.5 which is available under European Union Public Licence (https://pcse.readthedocs.io/en/stable/. Gridded daily temperature data as well as historical wheat harvest dates (name: 'wheat–grain harvest') to verify modeled harvest dates are available from the data portal of MeteoSwiss (https://www.meteoschweiz.admin.ch/service-und-publikationen/service/open-data.html). The daily MESHS data will be made available during 2026 on the same data portal. For access to the reconstructed hail time series in Switzerland please contact Lena Wilhelm (lena.wilhelm@unibe.ch). Wheat exposure layers are available from the Data API of the open-source risk modeling platform CLIMADA (name: 'crops CH wheat 1km') or Zenodo (https://doi.org/10.5281/zenodo.11064756).

Author contributions: RP: Conceptualization of the study, methodology, software, visualizations, paper writing, review and editing. LVG: development of wheat phenology modelling framework, paper writing and editing. LW: methodology, software, paper writing and editing. TS: software, paper writing and editing. LV: software, paper review and editing. PC: conceptualization, methodology, visualizations, paper review and editing. DF: provisioning of data from field trials, paper review

Acknowledgments: RP, TS, LV and LW acknowledge funding by the Swiss National Science Foundation (SNSF) Sinergia grant CRSII5_201792. LVG acknowledges funding of the SNSF for the project "PhenomEn" (grant number IZCOZ0_198091).

References

Ceglar, A., van der Wijngaart, R., de Wit, A., Lecerf, R., Boogaard, H., Seguini, L., … Baruth, B. (2019). Improving WOFOST model to simulate winter wheat phenology in Europe: Evaluation and effects on yield. *Agricultural Systems, 168*, 168–180. https://doi.org/10.1016/j.agsy.2018.05.002

Defila, C., Clot, B., Jeanneret, F., & Stöckli, R. (2016). Phenology in Switzerland since 1808. In S. Willemse, & M. Furger (Eds.), *From weather observations to atmospheric and climate sciences in Switzerland – Celebrating 100 years of the Swiss Society for Meteorology* (pp.291–306). Zurich: vdf. https://doi.org/10.3218/3746-3

Fossati, D., & Brabant, C. (2003). Die Weizenzüchtung in der Schweiz. *Agrarforschung Schweiz, 10*, 447–458. Retrieved from https://www.agrarforschungschweiz.ch/wp-content/uploads/2019/12/2003_1112_836.pdf

Frei, C. (2014). Interpolation of temperature in a mountainous region using nonlinear profiles and non-Euclidean distances. *International Journal of Climatology, 34*(5), 1585–1605. https://doi.org/10.1002/joc.3786

Graf, L. V. (2024). Prototyping of a Landscape-Scale Phenotyping Approach for Quantification of Winter Wheat Growth and Development Doctoral Thesis, ETH Zurich. https://doi.org/10.3929/ethz-b-000665050

Kopp, J., Schröer, K., Schwierz, C., Hering, A., Germann, U., & Martius, O. (2022). The summer 2021 Switzerland hailstorms: Weather situation, major impacts and unique observational data. *Weather, 78*(7), 184–191. https://doi.org/10.1002/wea.4306

Le Roux, R., Furusho-Percot, C., Deswarte, J. C., Bancal, M. O., Chenu, K., de Noblet-Ducoudré, N., … Launay, M. (2024). Mapping the race between crop-phenology and climate risks for wheat in France under climate change. *Scientific Reports, 14*(1), 8184. https://doi.org/10.1038/s41598-024-58826-w

Mallinson, H., Lasher-Trapp, S., Trapp, J., Woods, M., & Orendorf, S. (2024). Hailfall in a Possible Future Climate Using a Pseudo-Global Warming Approach: Hail Characteristics and Mesoscale Influences. *Journal of Climate, 37*(2), 527–549. https://doi.org/10.1175/JCLI-D-23-0181.1

Menzel, A., Sparks, T. H., Estrella, N., Koch, E., Aasa, A., Ahas, R., … Zust, A. (2006). European phenological response to climate change matches the warming pattern. *Global Change Biology, 12*(10), 1969–1976. https://doi.org/10.1111/j.1365-2486.2006.01193.x

Mo, F., Sun, M., Liu, X. Y., Wang, J. Y., Zhang, X. C., Ma, B. L., & Xiong, Y. C. (2016). Phenological responses of spring wheat and maize to changes in crop management and rising temperatures from 1992 to 2013 across the Loess Plateau. *Field Crops Research, 196*, 337–347. https://doi.org/10.1016/j.fcr.2016.06.024

Nisi, L., Martius, O., Hering, A., Kunz, M., & Germann, U. (2016). Spatial and temporal distribution of hailstorms in the Alpine region: A long-term, high resolution, radar-based analysis. *Quarterly Journal of the Royal Meteorological Society, 142*(697), 1590–1604. https://doi.org/10.1002/qj.2771

Olesen, J., Børgesen, C., Elsgaard, L., Palosuo, T., Rötter, R., Skjelvåg, A., … van der Fels-Klerx, H. (2012). Changes in time of sowing, flowering and maturity of cereals in Europe under climate change. *Food Additives & Contaminants. Part A, Chemistry, Analysis, Control, Exposure & Risk Assessment, 29*(10), 1527–1542. https://doi.org/10.1080/19440049.2012.712060

Portmann, R., Schmid, T., Villiger, L., Bresch, D. N., & Calanca, P. (2024). Modelling crop hail damage footprints with single-polarization radar: The roles of spatial resolution, hail intensity, and cropland density. *Natural Hazards and Earth System Sciences, 24*(7), 2541–2558. https://doi.org/10.5194/nhess-24-2541-2024

Punge, H. J., Bedka, K. M., Kunz, M., & Reinbold, A. (2017). Hail frequency estimation across Europe based on a combination of overshooting top detections and the ERA-INTERIM reanalysis. *Atmospheric Research, 198*, 34–43. https://doi.org/10.1016/j.atmosres.2017.07.025

Raupach, T. H., Martius, O., Allen, J. T., Kunz, M., Lasher-Trapp, S., Mohr, S., … Zhang, Q. (2021). The effects of climate change on hailstorms. *Nature Reviews. Earth & Environment, 2*(3), 213–226. https://doi.org/10.1038/s43017-020-00133-9

Raupach, T. H., Soderholm, J., Protat, A., & Sherwood, S. C. (2023). An Improved Instability – Shear Hail Proxy for Australia. *Monthly Weather Review, 151*(2), 545–567. https://doi.org/10.1175/MWR-D-22-0127.1

Rezaei, E. E., Siebert, S., Hüging, H., & Ewert, F. (2018). Climate change effect on wheat phenology depends on cultivar change. *Scientific Reports, 8*(1), 4891. https://doi.org/10.1038/s41598-018-23101-2

Rogger, J., Hund, A., Fossati, D., & Holzkämper, A. (2021). Can Swiss wheat varieties escape future heat stress? *European Journal of Agronomy, 131*, 126394. https://doi.org/10.1016/j.eja.2021.126394

Schiesser, H. (1990). Hailfall: The relationship between radar measurements and crop damage. *Atmospheric Research, 25*(6), 559–582. https://doi.org/10.1016/0169-8095(90)90038-E

Schmid, T., Portmann, R., Villiger, L., Schröer, K., & Bresch, D. N. (2024). An open-source radar-based hail damage model for buildings and cars. *Natural Hazards and Earth System Sciences, 24*(3), 847–872. https://doi.org/10.5194/nhess-24-847-2024

Schroeer, K., Trefalt, S., Hering, A., Germann, U., & Schwierz, C. (2022). *Hagelklima Schweiz: Daten, Ergebnisse und Dokumentation. Technical Report 283, MeteoSwiss.* Available from: https://www.meteoschweiz.admin.ch/dam/jcr: 34ced296-fc89-4bf6–b697-50c7cff73a65/20230907_fachbericht_283_neu.pdf

Sheehan, H., & Bentley, A. (2021). Changing times: Opportunities for altering winter wheat phenology. *Plants, People, Planet, 3*(2), 113–123. https://doi.org/10.1002/ppp3.10163

Swiss Granum (2023). *Anbauflaechen 2023. Technical report* Available from: https://www.swissgranum.ch/fileadmin/user_upload/swiss-granum/dokumente/Marktzahlen/Inlandproduktion/2024-10-31_Anbauflaechen.pdf

Thurnherr, I., Cui, R., Velasquez, P., Wernli, H., & Schär, C. (2025). The effect of 3 °C global warming on hail over Europe. *Geophysical Research Letters, 52*(18), e2025GL114811. https://doi.org/10.1029/2025GL114811

Waldvogel, A., Federer, B., & Grimm, P. (1979). Criteria for the Detection of Hail Cells. *Journal of Applied Meteorology, 18*(12), 1521–1525. https://doi.org/10.1175/1520-0450(1979)0182.0.CO;2

Warren, R. A., Ramsay, H. A., Siems, S. T., Manton, M. J., Peter, J. R., Protat, A., & Pillalamarri, A. (2020). Radar-based climatology of damaging hailstorms in Brisbane and Sydney, Australia. *Quarterly Journal of the Royal Meteorological Society, 146*(726), 505–530. https://doi.org/10.1002/qj.3693

Wilhelm, L., Schwierz, C., Schröer, K., Taszarek, M., & Martius, O. (2024). Reconstructing hail days in switzerland with statistical models (1959–2022). *Natural Hazards and Earth System Sciences, 24*(11), 3869–3894. https://doi.org/10.5194/nhess-24-3869-2024

Wit, A., Boogaard, H., Fumagalli, D., Janssen, S., Knapen, R., Kraalingen, D., … Diepen, K. (2019). 25 years of the WOFOST cropping systems model. *Agricultural Systems, 168*, 154–167. https://doi.org/10.1016/j.agsy.2018.06.018

Witt, A., Eilts, M. D., Stumpf, G. J., Johnson, J. T., Mitchell, E. D. W., & Thomas, K. W. (1998). An Enhanced Hail Detection Algorithm for the WSR-88D. *Weather and Forecasting, 13*(2), 286–303. https://doi.org/10.1175/1520-0434(1998)0132.0.CO;2

Manuscript received: December 1, 2024
Revisions requested: June 28, 2025
Revised version received: August 12, 2025
Manuscript accepted: October 6, 2025